Biology Direct

RESEARCH

Open Access

Integrating Circle-Seq with transcriptomics reveals genome-wide characterization of extrachromosomal circular DNA for dilated cardiomyopathy

Zhenhao Lin[1], Fangjie Dai[2], Bo Li[3,4], Yongchao Zhao[5,6*] and Changqian Wang[1*]

Abstract

Background Extrachromosomal circular DNAs (eccDNAs) are commonly found in various tumors and play a critical role in promoting oncogenesis. However, little is known about the characteristics and nature of eccDNAs in human heart failure. The aim of this study was to comprehensively analyze eccDNAs in human heart failure caused by dilated cardiomyopathy (DCM) and explore their potential functions.

Methods Circle-Seq and RNA-Seq were performed in cardiac tissue samples obtained from patients with DCM and healthy controls to identify eccDNAs and corresponding genes. Inward PCR, outward PCR and Sanger sequencing were conducted to validate the circular structure of eccDNAs. Bioinformatics was employed to probe the transcriptional activity of eccDNAs and their potential roles in the development of DCM. Ligase assisted minicircle accumulation strategy was used to synthesize a 500 bp circular DNA with a random sequence.

Results EccDNAs originated from all chromosomes, with the majority being less than 1 kb in size and about half containing genes or gene fragments. They were derived from specific repeat elements and primarily mapped to 5′UTR, 3′UTR, and CpG islands. Gene-rich chromosomes 17 and 19 exhibited higher eccDNA enrichment. Sequence motifs flanking eccDNA junction sites displayed frequent nucleotide repeats. The circular structure of eccDNAs were confirmed. Integration of Circle-Seq and RNA-Seq data identified that large eccDNAs can be directly transcribed in non-dividing cardiomyocytes, indicating their potential roles in gene expression. Small circular DNA elicited a stronger cytokine response than linear DNA with the same sequence.

Conclusions Our work provided a detailed profiling of eccDNAs in both healthy and DCM hearts and demonstrated the potential functions of both large and small eccDNAs. These findings enhance the comprehension of the role of eccDNAs in cardiac pathophysiology and establish a theoretical foundation for future investigations on eccDNAs in DCM.

Keywords Extrachromosomal circular DNA, Circle-Seq, RNA-Seq, Heart failure, Dilated cardiomyopathy

*Correspondence:
Yongchao Zhao
zhaoyc3988@126.com
Changqian Wang
wangcq1218@sh9hospital.org.cn
Full list of author information is available at the end of the article

Background

Extrachromosomal circular DNAs (eccDNAs) have been known for over half a century, but it is only in recent years that researchers have started to focus on their specific generation mechanisms and functions [1, 2]. Recent studies have highlighted their crucial roles in various biological processes, particularly in the context of cancer. Due to their elevated chromatin accessibility, eccDNAs carrying oncogenes can undergo more amplification compared to chromosomal genes [3]. Furthermore, eccDNAs can emerge early in the transition from high-grade dysplasia to cancer and promote tumor progression [4, 5]. Additionally, due to the absence of centromeres, eccDNAs can be randomly distributed to the daughter cells and integrate into linear genomes. These unique characteristics enable eccDNAs to remodel genomes and facilitate tumor adaption and evolution [6, 7]. EccDNA can also participate in the aging process and generate non-promoter-dependent RNAs that modulate gene expression [8–10]. Initially, eccDNAs were considered as by-products of replication failure. However, subsequent research revealed that eccDNA generation could be increased by apoptosis inducers, which rely on DNase γ-induced apoptotic DNA fragmentation, subsequently followed by DNA ligase 3-mediated ligation [11]. Another study reported that alternative end-joining (alt-EJ) drives the replication of retrotransposon DNA, leading to eccDNA production and mobilization from retrotransposons [12]. Although numerous hypotheses have been proposed for the formation mechanism of eccDNAs, the specific mechanisms responsible for eccDNA biogenesis remain elusive.

Dilated cardiomyopathy (DCM) is a prevalent global condition that results in heart failure, characterized by systolic dysfunction and ventricular dilation. The etiology of DCM involves a range of factors, including gene mutations, metabolic abnormalities, coronary artery disease and autoimmunity [13]. However, the exact molecular mechanisms underlying DCM remain unclear. Currently, the management of DCM remains challenging, and the mortality associated with this condition continues to escalate [13]. Therefore, it is crucial to identify potential therapeutic targets for DCM. Genetic variations have long been considered closely related to DCM, with many genes found to be associated with the condition. However, gene mutations alone do not fully explain the mechanisms underlying DCM development [14]. EccDNAs, a unique class of DNA, have the potential to harbor multiple genes or regulatory elements that may contribute to DCM development. Furthermore, owing to their circular structure, eccDNAs exhibit enhanced stability and accessibility.

Until recently, limited or no investigations have been conducted regarding the role of eccDNAs in cardiovascular diseases. A previous study reported a decrease in repetitive elements of eccDNAs with age in mouse hearts, suggesting their potential involvement in age-related heart diseases [15]. As the expression of eccDNA in human heathy and DCM heart still remains unclear, this study aims to provide a genome-wide profiling of eccDNAs in heart samples from both control subjects and DCM patients using Circle-Seq. Our findings not only offer a comprehensive landscape of eccDNAs in healthy and DCM hearts, but also demonstrate their transcriptional activity and significant involvement in the pathogenesis of DCM. These findings provide valuable insights into the genomic characteristics of the human heart.

Materials and methods

Clinical samples collection

Heart tissue samples were obtained from male healthy donors (specifically, the left ventricular wall of accident victims) and male patients diagnosed with DCM (specifically, the left ventricular wall of explanted hearts). Clinical data are presented in Supplementary Table 1.

eccDNA purification and Circle-Seq

Purification and amplification of eccDNAs from healthy and DCM heart samples were performed according to a previously reported protocol with slight modifications [16]. In brief, heart tissue samples were suspended in L1 buffer (Plasmid Mini AX; A&A Biotechnology) containing Proteinase K (Thermo Fisher, Waltham, MA, USA) and incubated overnight at 50 °C for digestion. After digestion, the samples underwent alkaline treatment and column purification as instructed by the Plasmid Mini AX kit. The resulting purified DNA samples were then digested with FastDigest MssI (Thermo Fisher) at 37 °C for 16 h to cut mitochondrial circular DNA. Exonuclease digestion with Plasmid-Safe ATP-dependent DNase (Epicentre, Madison, WI, USA) was carried out at 37 °C for 1 week. Enzyme and ATP were replenished daily with 30U and in the appropriate proportions, respectively, following the manufacturer's instructions, to completely remove any remaining linear DNA. The column-purified samples were utilized as templates for eccDNA amplification using the REPLI-g Midi Kit with phi29 polymerase. The amplified DNA was fragmented using a Bioruptor sonicator and then prepared for library construction using the NEBNext® Ultra II DNA Library Prep Kit. The libraries were subjected to high-throughput sequencing on an Illumina NovaSeq 6000 platform in the 150 bp paired-end mode. The DNA quality control report is

provided in Supplementary Table 2. The Circle-Seq was performed by CloudSeq Biotech Inc. (Shanghai, China).

RNA isolation and RNA-Seq

Total RNA was extracted using TRIzol and further purified with the RNeasy Mini Kit (Qiagen, Germany) according to the manufacturer's instructions. The RNA quality control report can be found in Supplementary Table 3. According to the manufacturer's instructions, rRNA removal from total RNA was accomplished using the NEBNext® rRNA Depletion Kit (New England Biolabs, Ipswich, MA, USA). The subsequent construction of the RNA-seq library employed the TruSeq Stranded Total RNA Library Prep Kit (Illumina, San Diego, CA, USA) with rRNA-depleted RNAs. Library quality control and quantification were conducted using the BioAnalyzer 2100 instrument (Agilent Technologies, Santa Clara, CA, USA). Sequencing of the library was performed on the Illumina NovaSeq 6000 platform using 150 bp paired-end mode.

Circle-Seq data and RNA-Seq data analysis

The analysis of Circle-Seq data was conducted following established protocols [10, 16]. Briefly, paired-end reads were harvested from Illumina NovaSeq 6000 sequencer, and were quality controlled by Q30. After 3′ adaptor-trimming and low-quality reads removing by Cutadapt software (v1.9.1), the high-quality clean reads were aligned to the reference genome (UCSC hg19) with BWA software (v0.7.12). The number of sequenced reads can be found in Supplementary Table 4. Then, Circle-map software (v1.1.4) was used to detect eccDNA within all samples, and Samtools (v1.7) software was used to get raw soft-clipped read counts of the break point. To determine the true positive of real circles versus background noise, some filtering parameters were used as follows: (1) Split reads ≥ 5; (2) Circle score ≥ 50; (3) Coverage increase in the start coordinate ≥ 0.33; (4) Coverage increase in the end coordinate ≥ 0.33; (5) Coverage continuity < 0.5. Normalization and identification of differentially expressed eccDNAs (Fold change ≥ 2 or ≤ 0.5 and P value < 0.05) were performed using EdgeR software (v3.32.1). Annotation of eccDNAs and mapping of read counts to repetitive elements were determined using Bedtools software (v2.30.0). Additionally, Bedtools software was employed to extract 10 bp upstream and downstream DNA sequences of eccDNA junction sites. GO and KEGG pathway enrichment analysis were carried out using the ClusterProfiler (v4.4.2) R package, and eccDNAs were visualized using IGV software (v2.14.1).

The analysis of RNA-Seq data was performed following a published study [17]. Briefly, high-quality reads were aligned to the human reference genome (UCSC hg19) using hisat2 software (v2.0.4). The Cuffdiff software (v2.2.1, part of cufflinks) was applied with guidance from the gtf gene annotation file to calculate the FPKM (Fragments per kilobase of exon per million fragments mapped) values for mRNA.

Validation for circular structure of eccDNAs

Specific primers were designed for outward PCR targeting the junction sites of eccDNAs. Genomic DNA and phi29 amplified products were used as templates. Inward PCR reactions were employed as positive controls for both circular and linear DNA templates. Each 10 μL PCR typically included 150 ng phi29-amplified template (2 μL), 10 μM primer, and 2×Master Mix (5 μL), and the PCR assay was performed for 40 cycles in a PCR cycler under standard PCR conditions. A combination of all group samples was used for all the PCR reactions. The PCR products were analyzed by agarose gel electrophoresis. Sanger sequencing was performed on the outward PCR products to validate the junction sites of eccDNAs. The PCR primers can be found in Supplementary Table 5.

Synthesis and transfection of small circular DNAs

The sequence of small circular DNA was generated using a "Random DNA sequence generator" tool (http://www.faculty.ucr.edu/~mmaduro/random.htm) with a 50% GC content. The ligase assisted minicircle accumulation (LAMA) strategy, as previously described, was utilized for the synthesis procedure [10]. The template sequences and their amplification primers are provided in Supplementary Table 6. For the LAMA reaction, equal amounts of template 1 and 2 amplification products were mixed with Taq DNA ligase (NEB) and buffer. The reaction was performed in thermocyclers using the following cycles: 95 °C for 3 min, 60 °C for 10 min, and 37 °C for 5 min, repeated for at least 15 cycles. Plasmid-Safe ATP-dependent DNase (Lucigen, Madison, WI, USA) was used to eliminate remaining linear DNAs from the LAMA reaction products. The circularized products were then recovered using a PCR Purification Kit (Qiagen). Inward PCR, outward PCR, and Sanger sequencing were performed to confirm the circular structure of the synthetic circular DNA. HL-1 cardiomyocytes and RAW 264.7 macrophages were cultured in DMEM culture medium supplemented with 10% fetal bovine serum (FBS) (Gibco, Carlsbad, CA, USA) and 1% penicillin/streptomycin (Invitrogen, Carlsbad, CA, USA) at 37 °C with 5% CO_2 and maximum humidity. The synthetic circular DNA was transfected into cells using the lipofectamine2000 (Invitrogen) in 24-well plate following the manufacturer's instruction. Briefly, 60,000 cells were seeded in a well of the 24-well plate 1 day before transfection. For each transfection, the 50 μL mixture consisted

of 500 ng synthetic eccDNA, 0.75 μL lipofectamine2000 and supplemented with opti-M (Invitrogen). Each transfection in one group was performed in at least triplicate. The cells were harvested for subsequent analysis 48 h after transfection. As a control, linear template DNAs (same sequence as synthetic circular DNA) were also transfected.

RT-qPCR assay of mRNA

All transfected cells were lysed using TRIzol for RNA isolation. The extracted RNA was then reverse transcribed into complementary DNA (cDNA) using the PrimeScript RT Reagent Kit (TaKaRa, Japan), following the manufacturer's instructions. The cDNA samples were subjected to qPCR analysis using an Applied Biosystems 7500 Fast Real-Time PCR system. The relative expression levels were calculated using the $2^{-\Delta\Delta CT}$ method. The qPCR primers for mRNA amplification can be found in Supplementary Table 7.

Statistical analysis

Quantitative data are presented as mean ± SEM. Normal distribution and homogeneity of variance were assessed for data comparison using Student's t-test or ANOVA. Nonparametric tests were used for data that did not follow a normal distribution. Correlation comparisons within each group were performed using either the Pearson or Spearman correlation test. Statistical analysis was conducted using GraphPad Prism 8 (GraphPad Software). A P value < 0.05 was considered statistically significant.

Results

Circle-Seq method for mapping eccDNAs

The Circle-Seq method was applied to comprehensively detect eccDNAs in both healthy and DCM heart samples. The main steps of the method are illustrated in Fig. 1A, and the log-scale distribution of paired-end reads from all chromosomes is displayed in Fig. 1B. In total, we detected 7879 eccDNAs across all samples, with 6549 identified in the control group and 5405 in the DCM group. Most of these eccDNAs were found in multiple samples (Fig. S1A, B). The sizes of the eccDNAs ranged from 0.01 to 10,000 kb, with the majority falling between 0.1 and 1 kb (Fig. 1C, D). Notably, there are two distinct peaks observed between 0.1 and 1 kb. The detected eccDNAs showed a seemingly random distribution across all chromosomes in both DCM and control groups (Fig. 1E, F). Additionally, the DCM group exhibited a lower number of eccDNAs derived from the same chromosome compared to the control group, except for the Y chromosome (Fig. S1C). Furthermore, we conducted an analysis of the breakpoints of eccDNAs in both groups and mapped their coordinates to the linear genome. The chromosomal distribution patterns of breakpoints were also similar between the control and DCM groups (Fig. S1D, E), suggesting that there is no difference in genomic stability between the two groups.

Genome-wide characterization of eccDNAs

Based on the genes or gene fragments associated with eccDNAs, the possible generation mechanism of eccDNAs is illustrated in Fig. 2A. Examples demonstrating the generation of eccDNAs are shown in Fig. 2B and Fig. S2A. Figure 2B displays the log-scale read coverage at the COBLL1 gene across all heart samples, revealing the presence of two COBLL1-associated eccDNAs, namely COBLL1$^{\text{circle exon 1}}$ and COBLL1$^{\text{circle exon 17}}$. Figure S2A displays the log-scale read coverage of a specific region on chromosome 10 across all heart samples, showing the presence of two eccDNAs derived from different genes in this region, namely SLC18A3$^{\text{circle exon 1}}$ and CHAT$^{\text{circle intron 1}}$.

We then investigated the relationship between protein-coding genes and eccDNAs in the two groups (Figs. 2C and S2B). Based on the mechanism of generation, eccDNAs have the capability to align with one or multiple protein-coding genes. In the control group, we found 3454 types of eccDNAs carrying no genes and 3086 types of eccDNAs carrying one or more genes. In the DCM group, we found 2847 types of eccDNAs carrying no genes and 2557 types of eccDNAs carrying one or more genes. Furthermore, eccDNAs can also map to one or more exons of a specific protein-coding gene according to the generation mechanism. In the control group, we identified 4890 genes generating only one eccDNA and 1596 genes generating two or more eccDNAs. In the DCM group, we identified 4103 genes generating only

(See figure on next page.)

Fig. 1 Circle-Seq method for mapping eccDNAs. **A** Schematic to illustrate Circle-Seq. EccDNAs are separated, purified and rolling circle amplified from all healthy and DCM heart samples. Detection of eccDNAs is based on split reads and discordant reads (grey arrows, concordant reads; red arrows, split reads; blue arrows, discordant reads). **B** Read coverage display (log-scale) at all chromosomes from all heart samples. **C**, **D** Size distribution of eccDNAs in control and DCM groups. Individuals are illustrated by different shapes respectively. Size of eccDNAs ranged from 0.01 kb to 10,000 kb. **E, F** Chromosomal distribution of detected eccDNAs in control and DCM groups

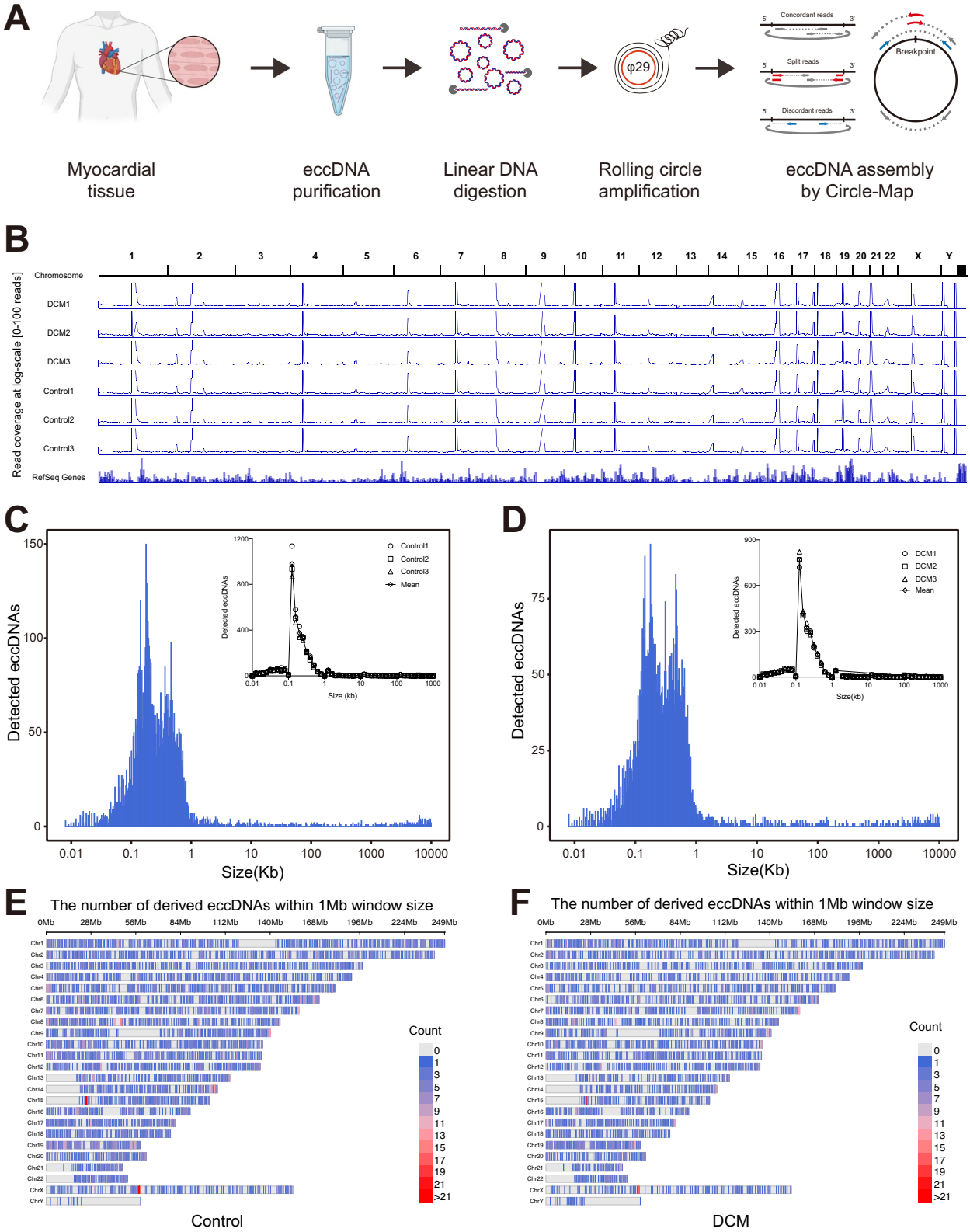

Fig. 1 (See legend on previous page.)

one eccDNA and 1372 genes generating two or more eccDNAs.

To understand the genomic origin of eccDNAs, we performed mapping analysis of all identified eccDNAs to various classes of genomic elements (Figs. 2D and S2C) as well as repetitive elements (Fig. 2E). EccDNAs were particularly enriched in CpG islands, 5′UTRs, and 3′UTRs, as well as repetitive elements including LINEs, SINEs, and satellites, suggesting a preferential generation of eccDNAs in these regions in heart tissues.

EccDNA frequency relative to chromosome and gene density

We further investigated the frequency of eccDNA generation from each chromosome. Interestingly, Chromosomes 17 and 19, which are known for their high gene density, exhibited a respective 1.3-fold and 2.0-fold higher average frequency of eccDNAs per Mb compared to other chromosomes. In contrast, the gene-poor chromosome Y displayed a 4.5-fold lower average frequency of eccDNAs per Mb (Fig. 3A). Subsequently, we categorized eccDNAs into two groups: eccDNAs with protein-coding genes and eccDNAs without protein-coding genes. Specifically, eccDNAs that contain complete genes or specific gene fragments are classified as eccDNAs with protein-coding genes. The gene-rich chromosomes 17 and 19 still exhibited a higher average frequency of eccDNAs with protein-coding genes per Mb compared to other chromosomes (Fig. 3B). However, the frequency of eccDNAs without protein-coding genes generation from each chromosome was similar (Fig. 3C). Additionally, there were no significant differences in the distribution of eccDNAs with or without protein-coding genes on different chromosomes between the control and DCM groups. We observed a positive correlation between the frequency of eccDNAs and the number of protein-coding genes per Mb (Fig. 3D), and a stronger positive correlation between the frequency of eccDNAs with protein-coding genes and the number of protein-coding genes per Mb (Fig. 3E). However, there was no correlation between the frequency of eccDNAs without protein-coding genes and the number of protein-coding genes per Mb (Fig. 3F). These findings suggest that the transcription or other characteristics of protein-coding genes may play a significant role in the frequency of eccDNA formation.

Motif signature of eccDNA junction sites

The identification of sequence motifs flanking eccDNA junction sites can provide insights into the generation mechanism of eccDNAs. Therefore, we proceeded to characterize the composition features of the sequences flanking eccDNA junction sites to determine if there were any specific patterns in eccDNA formation. We conducted a comprehensive analysis of the deoxynucleotide composition surrounding the start and end positions of all identified eccDNAs, spanning 10 base pairs upstream and downstream of these sites (Fig. 4A). To visually represent the frequency of each deoxynucleotide at each position flanking the eccDNA junction sites, we employed a stacked histogram (Fig. 4B, C). Notably, the size of each base in the Figure correspond to the frequency of the corresponding deoxynucleotide at that specific position, creating a proportional representation. We observed a similar distribution pattern of sequence motifs flanking eccDNA junction sites in both the control and DCM groups. The deoxynucleotides dATP and dTTP accounted for a higher proportion in the deoxynucleotide composition flanking eccDNA junction sites (Fig. S3). Additionally, nucleotide repeats such as 'AAA' and 'TTT' exhibited a high frequency in the sequence motifs flanking eccDNA junction sites. These findings suggest that dATP and dTTP, as well as deoxynucleotide repeats, may contribute more significantly to the junction sites of eccDNA.

Validation for circular structure of eccDNAs

We selected three eccDNAs for validation: SRP68$^{\text{circle exon 12}}$ (chr17$^{\text{circle 74040862–74041637}}$), PSMG2$^{\text{circle exon 4}}$ (chr18$^{\text{circle 12717020–12718905}}$) and chr1$^{\text{circle 16376520–16386335}}$. Inward PCR and outward PCR were employed to confirm the presence of these selected eccDNAs. The PCR products were then subjected to gel electrophoresis on agarose gels (Fig. 5A–C). The outward PCR products were further analyzed using Sanger sequencing to validate the junction sites of the eccDNAs.

(See figure on next page.)

Fig. 2 Genome-wide characterization of eccDNAs. **A** Schematic to illustrate the possible generation mechanism of eccDNAs. **B** Read coverage (log-scale) display at COBLL1 gene from all heart samples. Two eccDNAs, COBLL1$^{\text{circle exon 1}}$ and COBLL1$^{\text{circle exon 17}}$, derive from COBLL1 gene. **C** The number of eccDNAs carrying different numbers of genes and the number of genes generating different numbers of eccDNAs in control and DCM groups. **D** Genomic distributions of eccDNAs in control and DCM groups. **E** Repetitive regions from total mapped reads for eccDNAs derived from each heart sample. CpG2kbU, 2 kb upstream of CpG islands; CpG2kbD, 2 kb downstream of CpG islands; Gene2kbU, 2 kb upstream of genes; Gene2kbD, 2 kb downstream of genes; LINE, long interspersed nuclear element; SINE, short interspersed nuclear element; rRNA, ribosomal RNA; snRNA, small nuclear RNA; tRNA, transport RNA; LTR, long terminal repeat

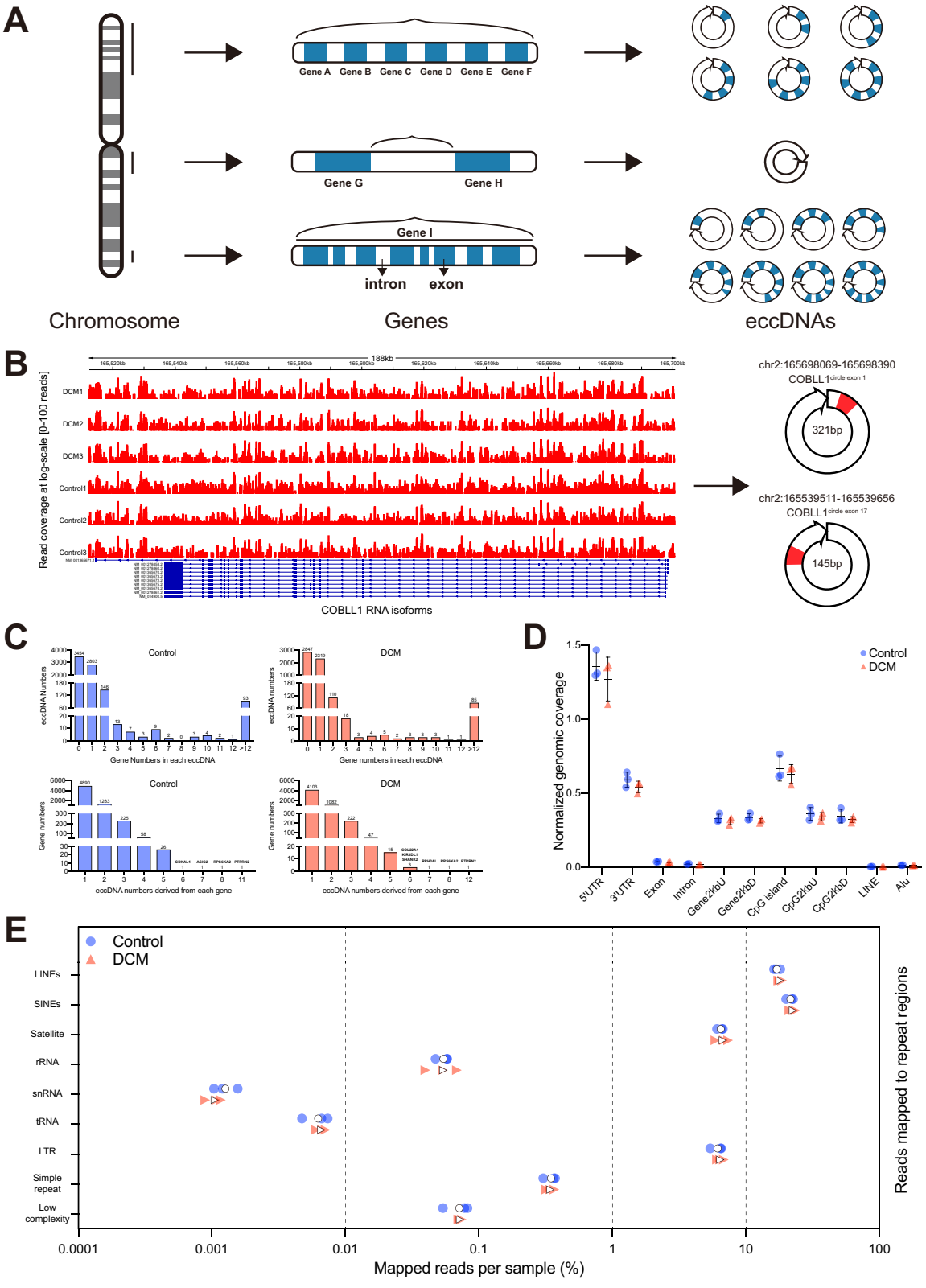

Fig. 2 (See legend on previous page.)

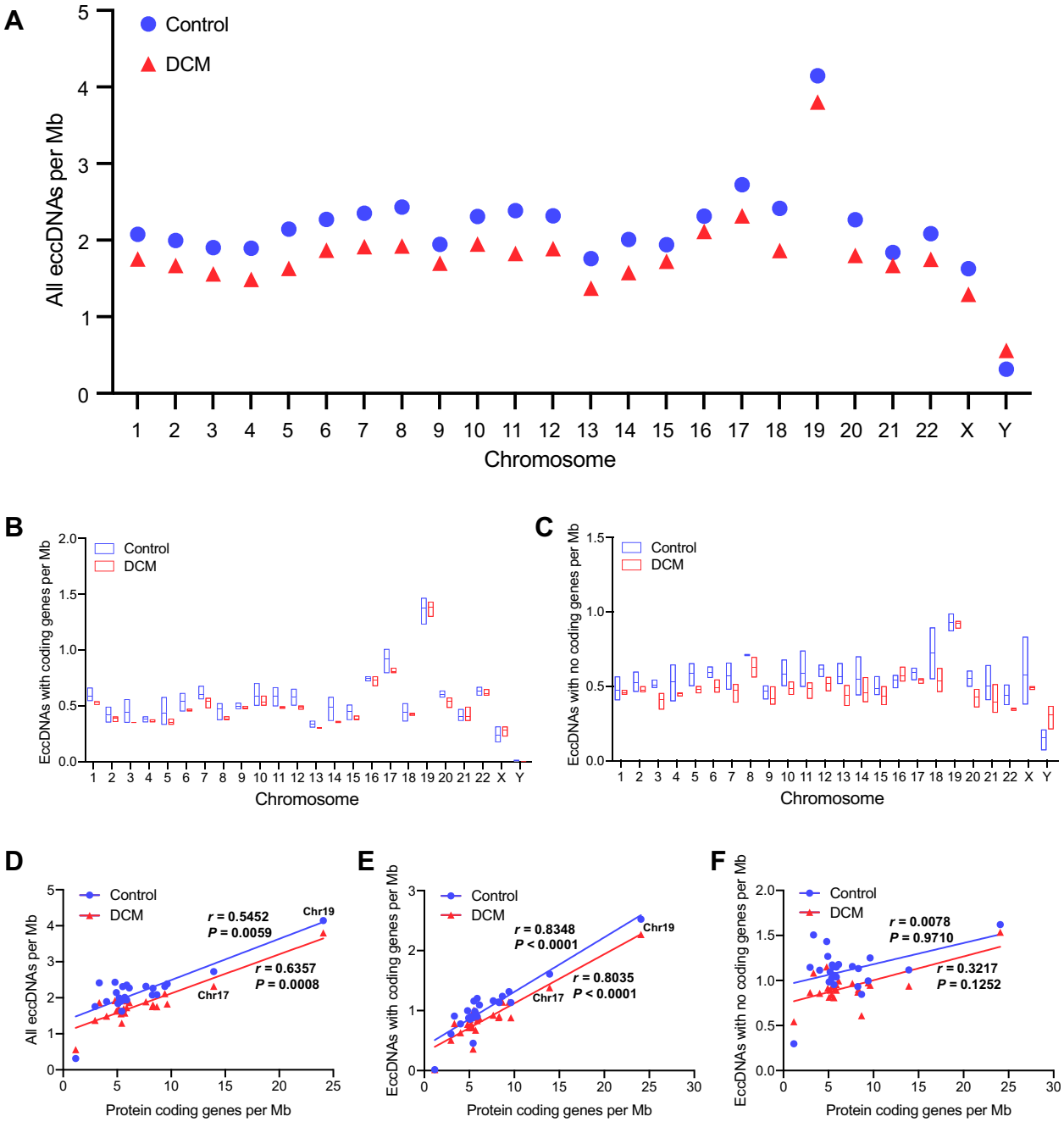

Fig. 3 EccDNA frequency relative to chromosome and gene density. **A** All eccDNAs per Mb from control (blue dot) and DCM (red triangle) groups per chromosome. **B** The number of eccDNAs with protein-coding genes is quantified and categorized by chromosome in control (blue box) and DCM (red box) samples. **C** The number of eccDNAs without protein-coding genes is quantified and categorized by chromosome in control (blue box) and DCM (red box) samples. **D** All eccDNAs per Mb from control (blue dot) and DCM (red triangle) groups per protein-coding genes per Mb (chromosome 17 and 19 are marked). **E** EccDNAs with protein-coding genes per protein coding genes per Mb (chromosome 17 and 19 are marked). **F** EccDNAs without protein-coding genes per protein coding genes per Mb

Integrated analysis of eccDNAs and mRNAs

Based on our results in Fig. 3, it appears that the transcription of protein-coding genes may impact the frequency of eccDNA biogenesis. To further investigate the relationship between eccDNAs and transcription, we performed RNA-Seq on heart samples from both control and DCM groups. To determine differentially expressed eccDNAs and mRNAs, we set the criteria as

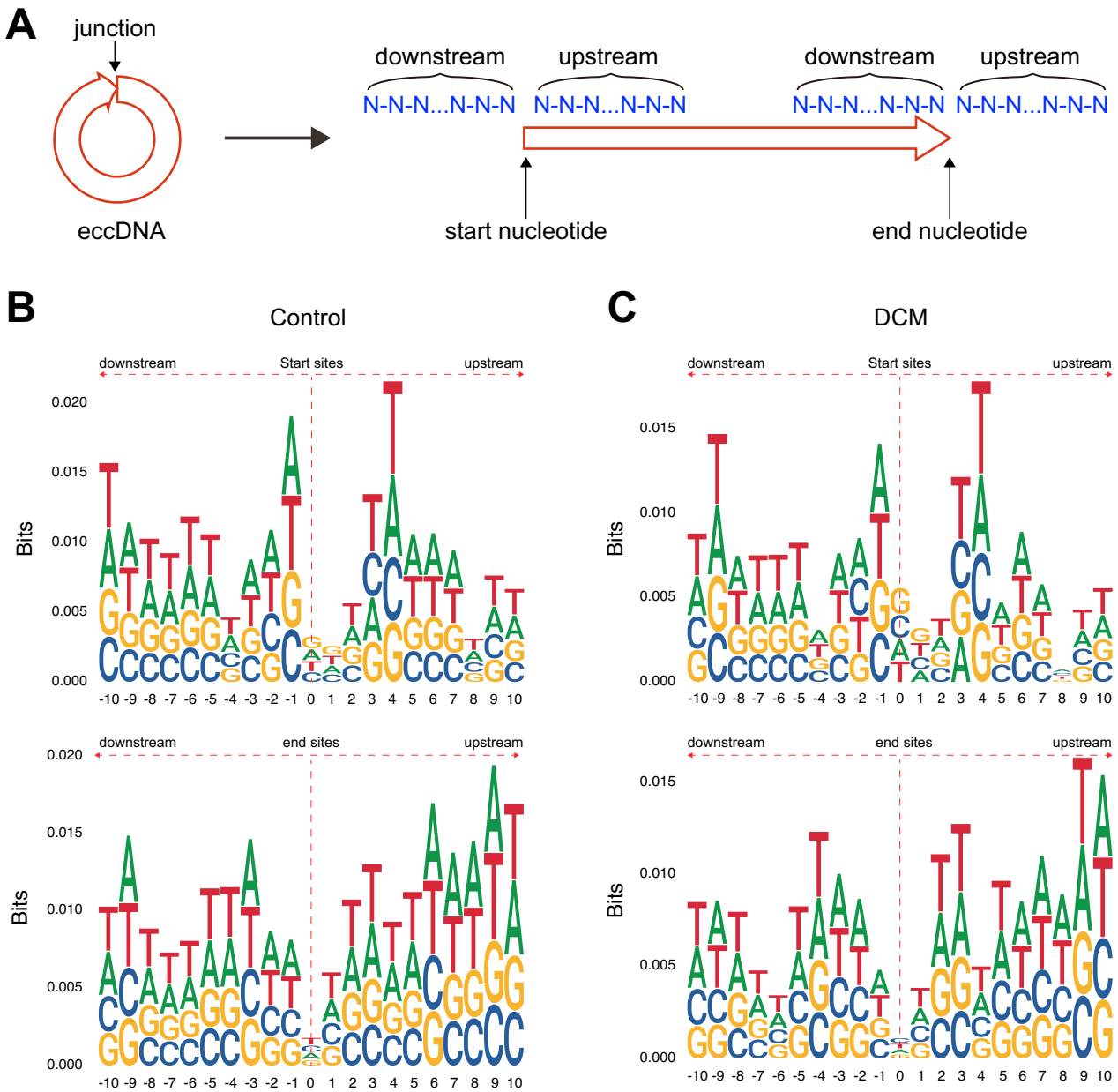

Fig. 4 Motif signature of eccDNA junction sites. **A** Schematic to illustrate deoxynucleotide composition flanking eccDNA junction sites. **B**, **C** The deoxynucleotide frequencies surrounding the junction sites of eccDNAs derived from control and DCM groups

a fold change of ≥ 2 or ≤ 0.5 and a *P* value of < 0.05. Heat maps depicting the dysregulated eccDNAs and mRNAs are presented in Fig. 6A, B, respectively. When comparing the DCM group to the control group, we identified 329 dysregulated eccDNAs, with 168 upregulated and 161 downregulated. Moreover, we observed 617 upregulated mRNAs and 1125 downregulated mRNAs in the DCM group (Supplementary Tables 8 and 9). Additionally, there were 303 protein-coding genes associated with upregulated eccDNAs, and 360 protein-coding genes associated with downregulated eccDNAs (Fig. 6C). Furthermore, by overlapping these protein-coding genes with dysregulated mRNAs, we identified 9 upregulated mRNAs potentially associated with upregulated eccDNAs and 33 downregulated mRNAs possibly associated with downregulated eccDNAs (Fig. 6D). The chromosomal locations of the upregulated eccDNAs and mRNAs are illustrated in Fig. 6E, while the downregulated eccDNAs and mRNAs are shown in Fig. 6F. It seems that the chromosomal distribution patterns of these dysregulated

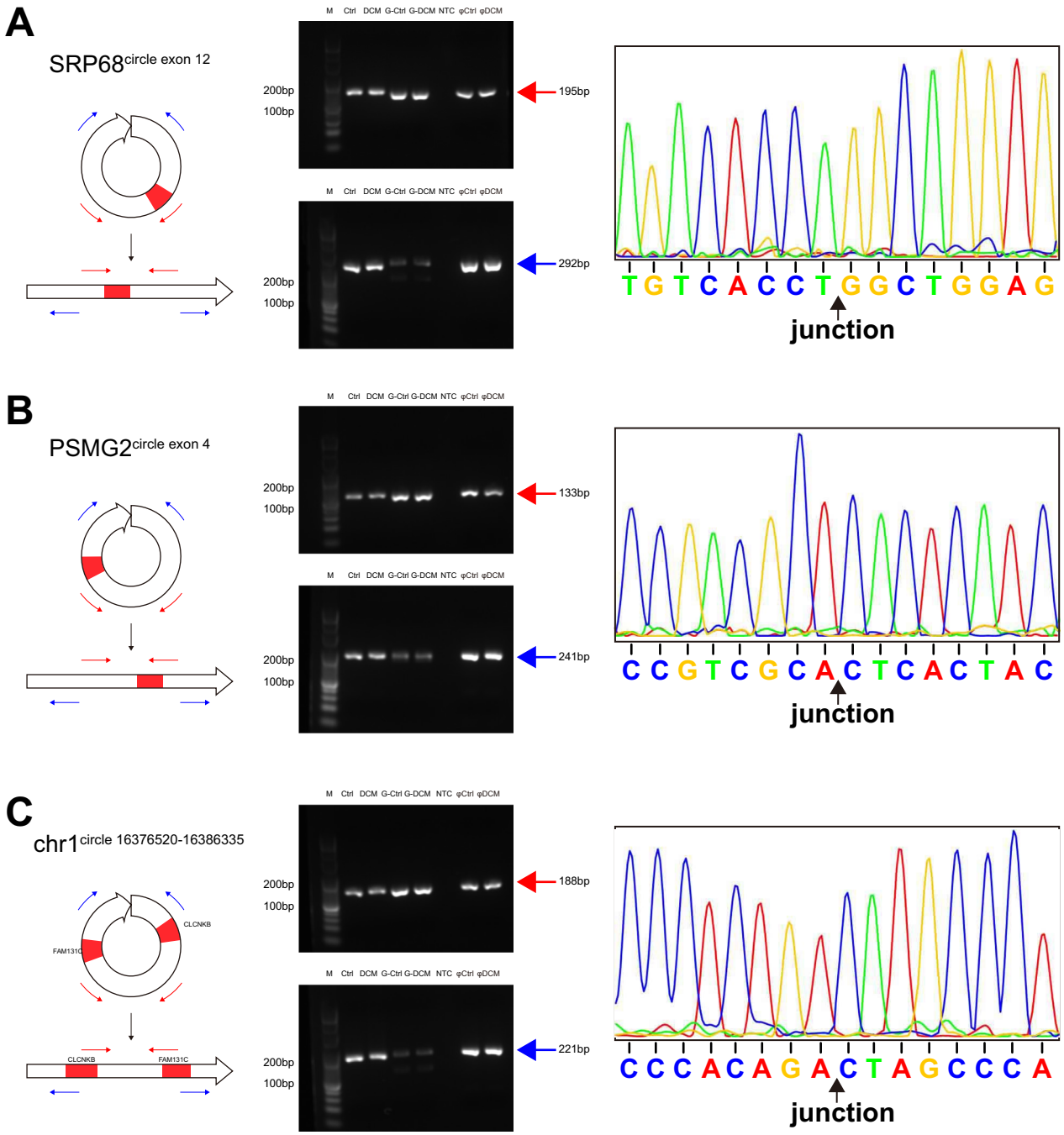

Fig. 5 Validation for circular structure of eccDNAs. Gel electrophoresis image for validated eccDNAs **A** SRP68$^{\text{circle exon 12}}$, **B** PSMG$^{\text{circle exon 4}}$ and **C** chr1$^{\text{circle 16376520–16386335}}$ by outward PCR (blue arrows) and inward PCR (red arrows). Outward PCR products are used for Sanger sequencing to validate the junction sites of eccDNAs. EccDNAs are named according to gene content or the location on the chromosome. Schematic diagrams are used to illustrate inward PCR and outward PCR. Red boxes: exons or genes; M: Marker; Ctrl: unamplified eccDNA of control samples; DCM: unamplified eccDNA of dilated cardiomyopathy samples; G-Ctrl: genomic DNA of control samples; G-DCM: genomic DNA of dilated cardiomyopathy samples; φCtrl: φ29 amplified eccDNA of control samples; φDCM: φ29 amplified eccDNA of dilated cardiomyopathy samples; NTC: non-template control

eccDNAs and mRNAs exhibit little similarity. A weak positive correlation was observed between the number of eccDNAs per gene and transcript level (Fig. 6G). However, a general correlation between the number of dysregulated eccDNAs per gene and transcript level was not found (Fig. 6H). These results suggest that some mRNAs may be transcribed either fully or partially from eccDNAs, in addition to the linear genomic DNA.

Gene Ontology (GO) analysis and Kyoto Encyclopedia of Genes and Genomes (KEGG) pathway analysis were conducted based on the dysregulated eccDNAs. The results of the GO analysis revealed a predominant association between dysregulated eccDNAs and biological processes and molecular functions pertaining to immune response, cytokine production, and cytotoxicity (Fig. 6I). The KEGG pathway analysis further demonstrated that the dysregulated eccDNAs were mainly enriched in pathways related to immune response, cytotoxicity, and cellular senescence (Fig. 6J). These results showed that genes associated with cytokine production and immune response contribute more to the formation of dysregulated eccDNAs, indicating their increased activity during the development of DCM. This notion was also confirmed by gene set enrichment analysis (GSEA) (Fig. S4).

EccDNA transcript from eccDNA$^{\text{circle KMT2C}}$

To investigate the possibility of mRNAs being transcribed directly from eccDNAs, we analyzed the sequences of mRNAs from all heart samples to identify any matching transcription events across the eccDNA junction sites. In the DCM3 heart sample, we observed the presence of the eccDNA$^{\text{circle KMT2C}}$, and two sequenced RNA reads perfectly overlapped with the split reads of the eccDNA$^{\text{circle KMT2C}}$ (Fig. 7A). Inward PCR and outward PCR were employed to confirm the circular structure of eccDNA$^{\text{circle KMT2C}}$ (Fig. 7B). The PCR products were then subjected to gel electrophoresis on agarose gels. The outward PCR products were further analyzed using Sanger sequencing to validate the junction sites of eccDNA$^{\text{circle KMT2C}}$ (Fig. 7C). This observation strongly suggests that these two RNA reads were transcribed directly from the eccDNA$^{\text{circle KMT2C}}$.

Functions of small eccDNAs

To further investigate the potential functions of small eccDNAs (< 1 kb), which constitute more than 95% of the identified eccDNAs and are not transcriptionally active, we employed the LAMA method to synthesize a 500 bp circular DNA with a random sequence (Fig. 8A). Inward PCR and outward PCR were employed to confirm the circular structure of the synthesized circular DNA (Fig. 8B). The PCR products were then subjected to gel electrophoresis on agarose gels. The outward PCR products were further analyzed using Sanger sequencing to validate the junction sites of the synthesized circular DNA (Fig. 8C). The synthesized circular DNA was then transfected into cardiomyocytes and macrophages respectively. Compared to linear DNA transfection, the synthesized circular DNA enhances cytokine production to a great extent (Fig. 8D).

Discussion

In recent years, increasing evidences indicate that eccDNAs are involved in normal cellular physiology, including homologous recombination, DNA damage repair and the production of short regulatory RNAs, highlighting the potential dysregulation of certain eccDNAs in the development of non-tumor diseases [10, 18, 19]. While eccDNAs have long been known to originate from the linear genome and exist in both normal and tumor tissues, their expression and characteristics in healthy and DCM heart samples have not yet been reported [20, 21]. Therefore, this study aimed to comprehensively investigate eccDNAs in human hearts and explore their potential implications in the pathogenesis of DCM.

Using Circle-Seq, we detected a total of 8152 eccDNAs in the control and DCM groups, with 168 eccDNAs upregulated and 161 eccDNAs down-regulated. Our data revealed a significant difference in the number of eccDNAs identified between cardiac tissue and tumor tissue, with a notably lower count observed in the former [22, 23]. This observation suggests a close association between eccDNA generation and cell division, which often results in double-stranded DNA breaks. Furthermore, it is worth noting that our study detected some non-unique eccDNAs, as shown in Fig. S1A, with 349

(See figure on next page.)

Fig. 6 Integrated analysis of eccDNAs and mRNAs. **A** Cluster heat map of dysregulated eccDNAs. **B** Cluster heat map of dysregulated mRNAs. **C** Summary data of dysregulated eccDNAs, mRNAs and dysregulated eccDNAs associated protein-coding genes. **D** Venn diagram shows the overlapping part of dysregulated mRNAs and dysregulated eccDNAs associated protein-coding genes. **E** The chromosomal location of upregulated eccDNAs (red circle) and mRNAs (red cross). **F** The chromosomal location of downregulated eccDNAs (blue circle) and mRNAs (blue cross). **G** EccDNA counts per gene relative to average transcription level of control (red cross) and DCM (blue cross) groups. **H** Dysregulated eccDNA counts per gene relative to average transcription level of control (red cross) and DCM (blue cross) groups. **I** GO enrichment analysis of dysregulated eccDNAs. **J** KEGG pathway enrichment analysis of dysregulated eccDNAs

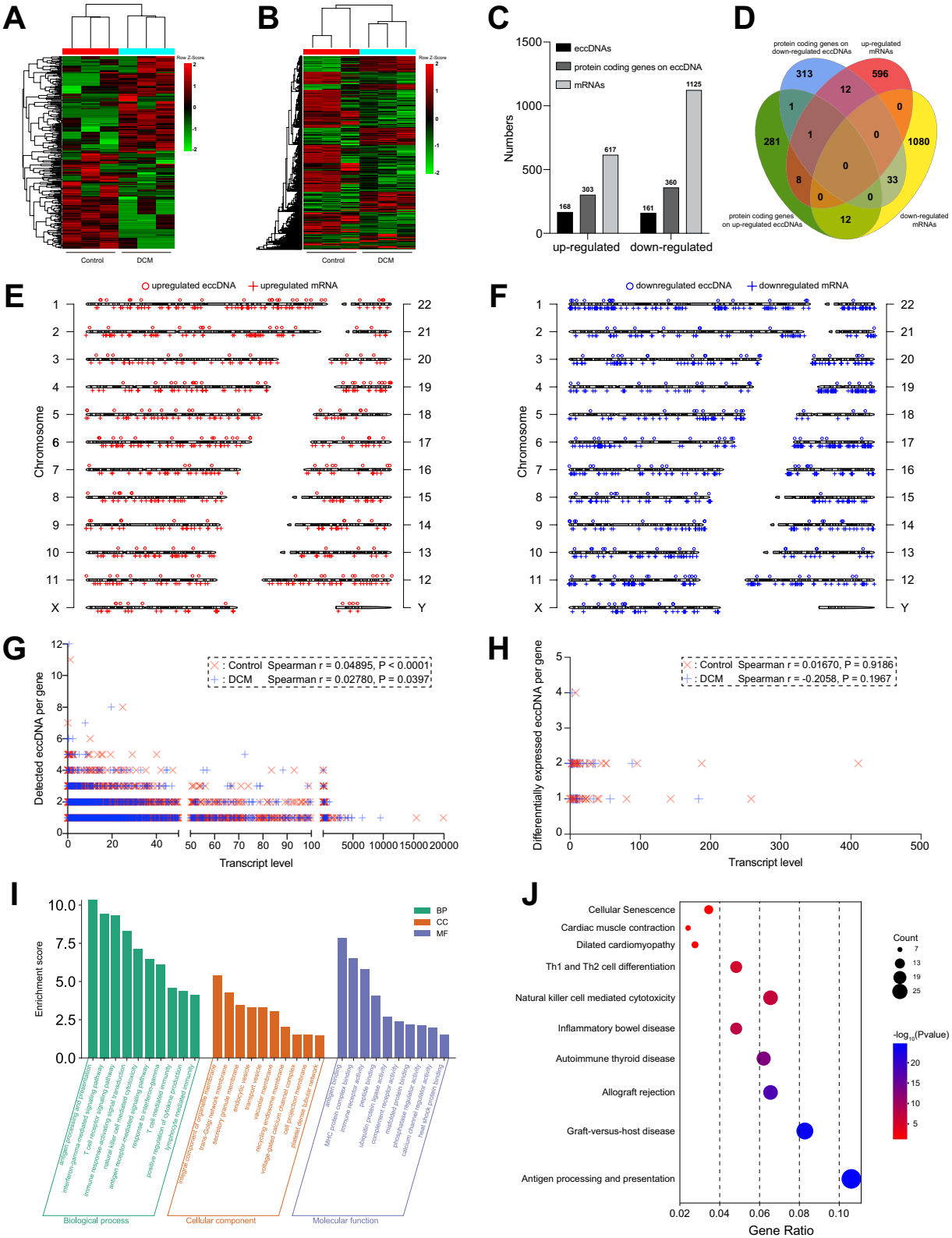

Fig. 6 (See legend on previous page.)

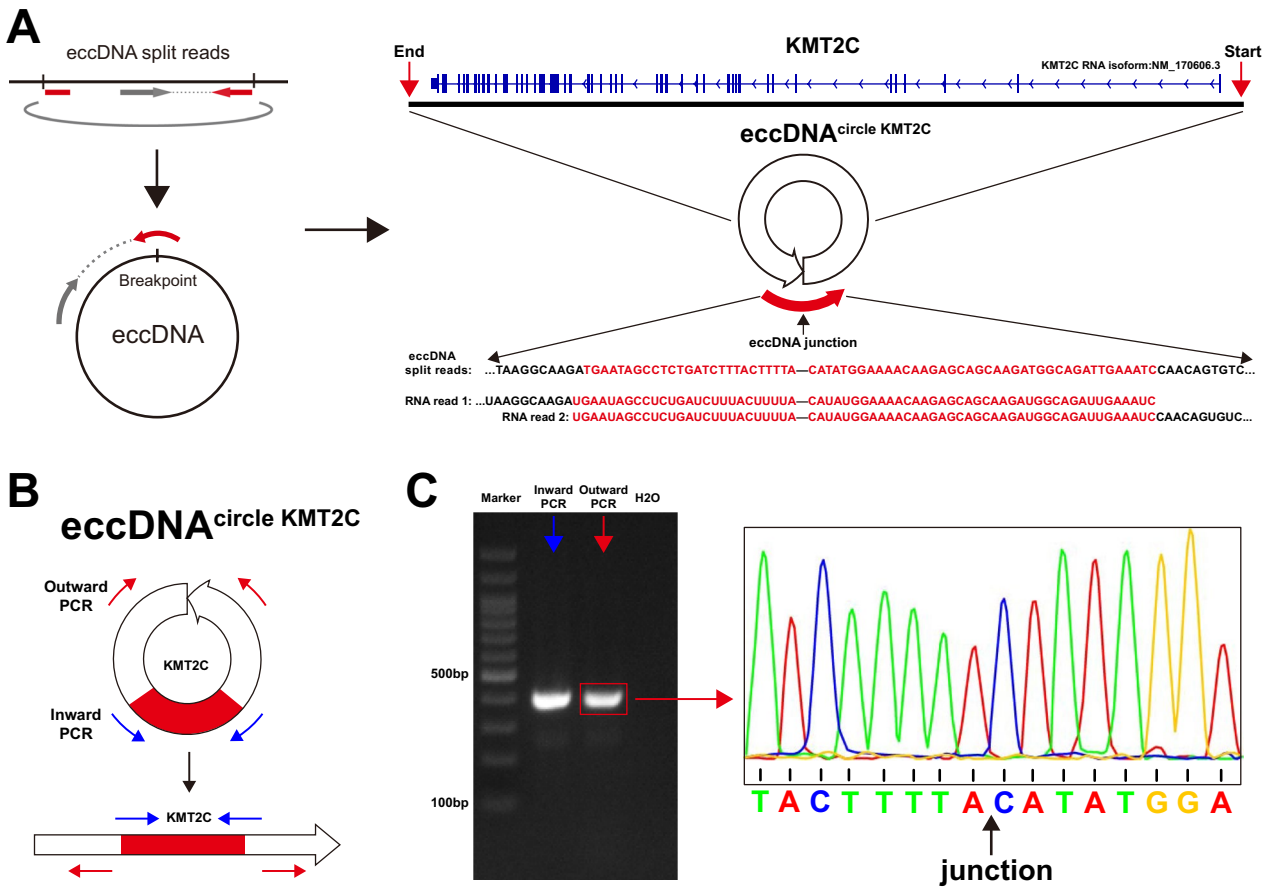

Fig. 7 EccDNA transcript from eccDNA$^{circle\ KMT2C}$. **A** The two sequenced RNA reads from DCM3 heart sample overlap perfectly to the split reads of eccDNA$^{circle\ KMT2C}$. The nucleotide sequence encompassing the eccDNA junction site is marked by red text. **B** Schematic diagram to illustrate the validation for circular structure of eccDNA$^{circle\ KMT2C}$. **C** Gel electrophoresis image for outward PCR and inward PCR products of eccDNA$^{circle\ KMT2C}$. Outward PCR products are used for Sanger sequencing to validate the junction sites of eccDNA$^{circle\ KMT2C}$

eccDNAs present in all samples. This substantial overlap between different samples is not so common. The heart belongs to a non-dividing system. If the generation of eccDNA is linked to cell division, these non-unique eccDNAs may remain in the heart post-development, indicating their potential role in heart physiology. Further research is required to validate this hypothesis. Several studies have proposed that eccDNA formation may be mediated by DNA damage repair mechanisms, such as microhomology-mediated end joining, homologous recombination and nonhomologous end joining [24–27]. While no significant difference in the size of eccDNAs were observed between the control and DCM groups, most eccDNAs were found to be less than 1 kb, exhibiting two distinct size distribution peaks that resemble a characteristic feature of muscle tissue, as previously reported [16]. Additionally, our data revealed a random mapping of all detected eccDNAs across all chromosomes in both groups. Although there was no specific hotspot for eccDNA formation in the human genome, chromosomes with a higher density of protein coding genes tended to contribute more frequently to eccDNA generation. Furthermore, we observed a positive correlation between the frequency of eccDNAs and the number of protein-coding genes per Mb, supporting previous findings and suggesting a strong link between gene transcription and eccDNA generation [28–30].

To investigate the origin of eccDNA in the genome, we mapped eccDNAs from the control and DCM groups to different classes of genomic elements. Our findings demonstrated a significant enrichment of eccDNAs in 5′UTR, 3′UTR and CpG islands, with no significant difference observed between the two groups in the terms of eccDNA origin. The 5′UTR and CpG islands have been identified as hotspots for R-loop structures, which activate mismatch repair pathways and contribute to eccDNA generation [19, 31, 32]. Additionally, previous research has highlighted an overrepresentation of 5′UTR and 3′UTR sequences in eccDNAs [24, 25]. Repetitive elements like SINEs, LINEs, and satellites have been

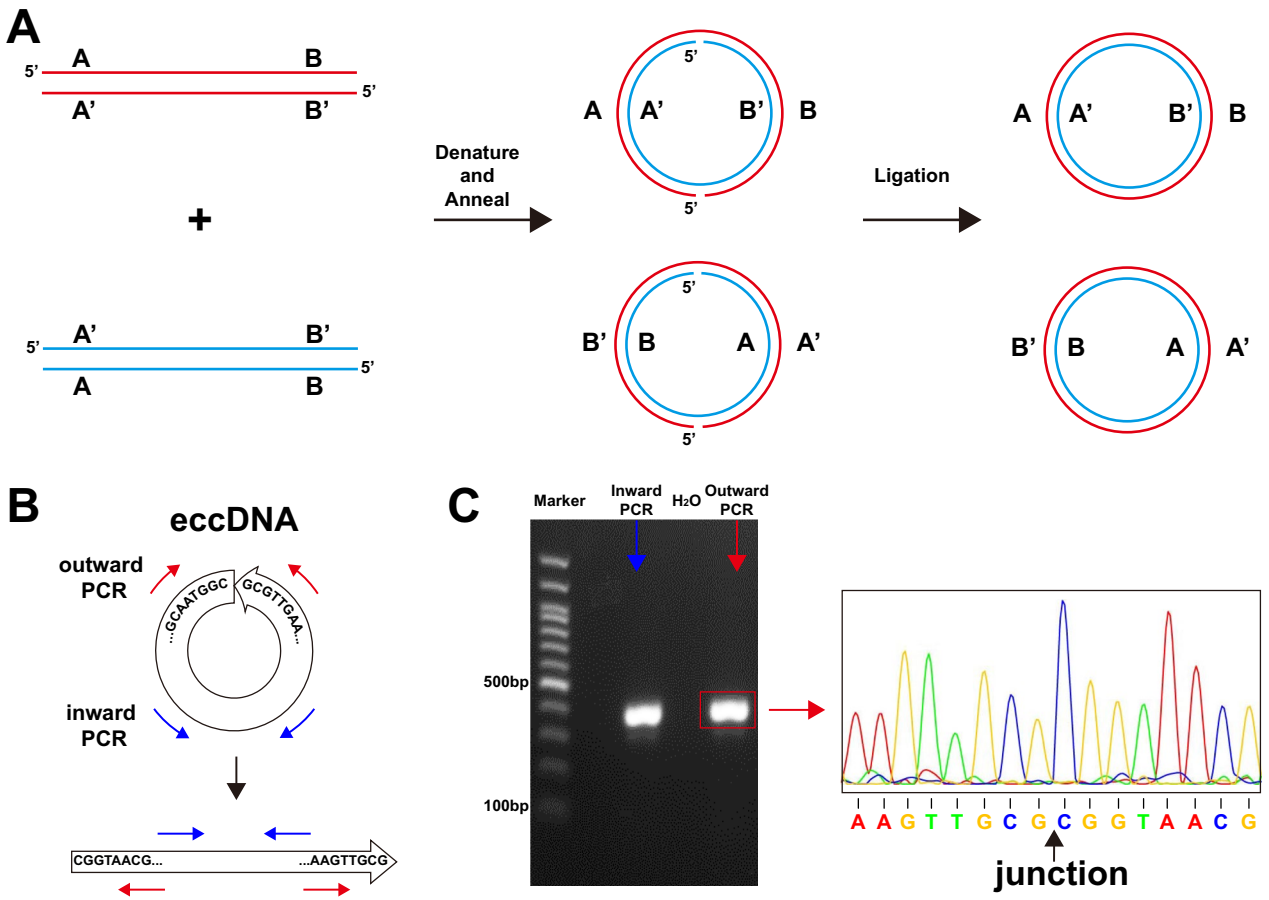

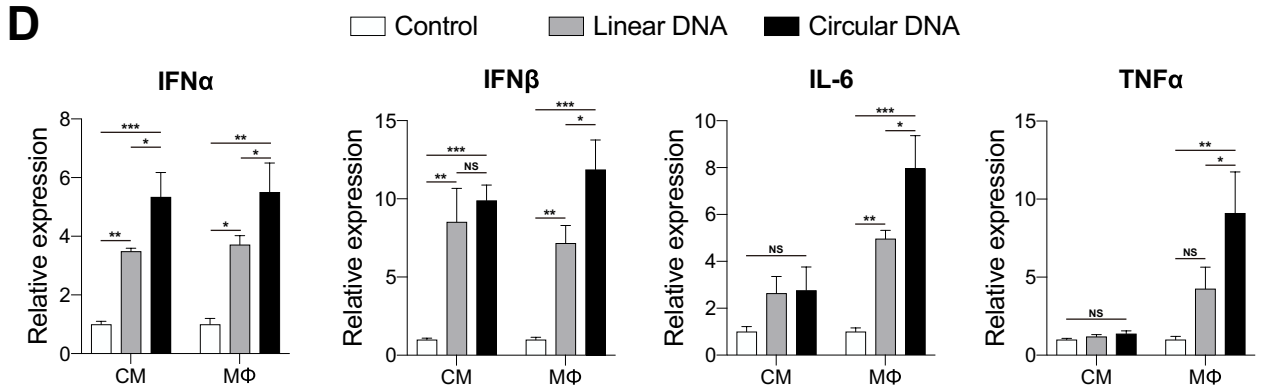

Fig. 8 Functions of small eccDNAs. **A** Diagram of synthetic circular DNA preparation by LAMA approach. **B** Schematic diagram to illustrate the validation for circular structure of the synthetic circular DNA. **C** Gel electrophoresis image for outward PCR and inward PCR products of the synthetic circular DNA. Outward PCR products are used for Sanger sequencing to validate the junction sites of the synthetic circular DNA. **D** Synthetic circular DNA induces a greater cytokine response in cardiomyocytes and macrophages (n = 3). The experiments were repeated for three times. CM, Cardiomyocyte; MΦ, Macrophage; NS, not significant; * $P < 0.05$, ** $P < 0.01$, *** $P < 0.001$

identified as significant contributors to eccDNA formation in the human genome [16, 22, 29]. Our data align with these findings and suggest a regional specificity in the process of eccDNA formation.

To gain further insights into the generation mechanism of eccDNA, we conducted an analysis of the deoxynucleotide composition flanking eccDNA junction sites, aiming to identify any potential motif patterns associated

with eccDNA formation. Previous studies have consistently reported the presence of nucleotide repeats near eccDNA junction sites, suggesting a potential correlation between these repeats and eccDNA generation [29, 33]. Our analysis further supports these findings by revealing a significant enrichment of nucleotide repeats in a large proportion of eccDNAs, particularly in the sequence motifs flanking the junction sites. This reinforces the idea that A/T may significantly contribute to the junction sites of eccDNA. Nucleotide repeats have been associated with DNA breakpoints and susceptibility sites for R-loop formation [16, 19, 28]. Moreover, the presence of microhomology sequences flanking eccDNA junction sites, indicated by these nucleotide repeats, suggests a potential role of microhomology in promoting eccDNA formation [34].

By integrating Circle-Seq and RNA-Seq data, we discovered a weak positive correlation between the number of eccDNAs per gene and the transcript level, as well as some transcription events occurring across the eccDNA junction sites. This suggests a potential role for eccDNAs in genetic transcription and translation processes. However, we matched the eccDNA split reads detected in each sample with the RNA reads detected in the same sample. Some samples did not have any matching items, while others only had a few matchable eccDNAs, the majority of which are over 200 kb. These results suggest that transcription from eccDNAs might be a rare event in the human heart. Our GO and KEGG pathway enrichment analyses have further demonstrated an increased involvement of genes related to cytokine production and immune response in eccDNA formation during DCM progression, indicating heightened activity of these genes. It is widely recognized that double-stranded DNA can directly trigger immune responses and inflammation, thereby contributing to the development of diseases [35]. Additionally, a previous study has demonstrated that eccDNAs, due to their circular structure, can act as immunostimulants [11]. Building upon these findings, we hypothesize that the majority of detected eccDNAs in our study, which are small and non-transcriptionally active, may activate immune response and inflammation by promoting cytokine production. To verify this hypothesis, we synthesized small circular DNA in vitro and transfected it into cardiomyocytes and macrophages. We found that circular DNA exhibited a stronger capacity to stimulate cytokine secretion compared to linear DNA.

This study had some limitations. First, the in vitro synthesized small circular DNA may not accurately replicate the in vivo eccDNA, as its spatial conformation might differ. Second, the synthesis efficiency of LAMA decreases significantly as the circular DNA length increases, making it challenging to study larger eccDNAs (> 1 kb) that are transcriptionally active. Third, due to the scarcity of human cardiac tissue samples, particularly those from healthy individuals, the sample size in this study was limited. Furthermore, cardiac tissue samples used in this study is somewhat homogeneous in terms of gender and race. Fourth, even though we have obtained that two RNA reads can perfectly match the split reads of eccDNA$^{\text{circle KMT2C}}$, it must be noted that this novel RNA transcript may derive from individual variations. Last, the exact mechanisms underlying eccDNA generation remain unclear, hindering functional experiments in vivo. Therefore, future research should focus on fundamental studies to unravel these mechanisms and develop improved techniques for deeper investigations into the association between eccDNAs and disease development.

Conclusions

Our study utilized Circle-Seq to investigate the genome-wide profile of eccDNAs in both healthy and DCM hearts, providing novel insights into their characteristics. We observed a diverse population of eccDNAs and characterized their features, including size distribution, chromosomal and genomic origins, as well as motif signatures. Furthermore, our work demonstrated the transcriptional activity of eccDNA$^{\text{circle KMT2C}}$ in the human heart, indicating the potential functional roles of large eccDNAs in gene expression. More importantly, we found that small eccDNAs might contribute to the development of DCM by promoting cytokine production and then triggering immune or inflammatory responses. These findings not only advance our understanding of eccDNAs in the human heart, but also provide a theoretical foundation for future investigations on their implications in DCM.

Abbreviations

alt-EJ	Alternative end-joining
Circle-Seq	Circular DNA sequencing
DCM	Dilated cardiomyopathy
eccDNAs	Extrachromosomal circular DNAs
GO	Gene oncology
GSEA	Gene set enrichment analysis
KEGG	Kyoto encyclopedia of genes and genomes
LAMA	Ligase assisted minicircle accumulation
LINEs	Long interspersed nuclear elements
PCR	Polymerase chain reaction
RNA-Seq	RNA sequencing
RT-qPCR	Reverse transcription-quantitative polymerase chain reaction
SINEs	Short interspersed nuclear elements
5′UTR	5′ untranslated region
3′UTR	3′ untranslated region

Supplementary Information

The online version contains supplementary material available at https://doi.org/10.1186/s13062-024-00556-0.

Additional file 1. Characteristics for eccDNA numbers and breakpoints. A Upset plot to illustrate the overlaps of eccDNAs derived from each heart

sample. The column at the bottom left shows the total eccDNAs derived from each heart sample. The black dots at the bottom right and the corresponding columns above represent the number of the eccDNAs that are not overlapped by other sets. The black dots with lines and corresponding columns above represent the number of overlapping eccDNAs of sets. B Summary data of eccDNA numbers derived from control and DCM groups. C Chromosomal distribution of detected eccDNAs in control and DCM groups. D, E Chromosomal distribution of eccDNA breakpoints in control (blue line) and DCM (red line) groups.

Additional file 2. Some genomic features of eccDNAs. A Read coverage (log scale)display at chromosome 10 (50818433 50818623). Two eccDNAs, SLC18A3$^{\text{circle exon1}}$ and CHAT$^{\text{circle intron 1}}$, derive from this region. B The number of eccDNAs with and without protein coding genes in control and DCM groups. C Statistical analysis of genomic distributions of eccDNAs. * P < 0.05, ** P <0.01, *** P < 0.001, **** P < 0.0001.

Additional file 3. Summary data of deoxynucleotides flanking eccDNA junction sites. A, B, C, D Statistical analysis of deoxynucleotide composition from 10 bp upstream to 10 bp downstream of the start and end position of eccDNAs.NS, not significant; ** P < 0. 01, **** P < 0.0001.

Additional file 4. Gene set enrichment analysis (GSEA) of eccDNAs. A, B, C The GSEA analysis of GO based on eccDNAs that highly expressed in DCM group. D The GSEA analysis of Reactome based on eccDNAs that highly expressed in DCM group.

Additional file 5. The clinical data of the heart samples.

Additional file 6. The DNA quality control report.

Additional file 7. The RNA quality control report.

Additional file 8. The number of sequenced reads for Circle-Seq.

Additional file 9. The PCR primers for outward and inward PCR.

Additional file 10. The template sequences and their amplification primers for LAMA.

Additional file 11. The qPCR primers for mRNA amplification.

Additional file 12. mRNA expression profiling.

Additional file 13. eccDNA expression profiling.

Acknowledgements
We would like to express our gratitude to Dr. Mingjie Chen from NewCore Biotech Co., Ltd. Shanghai, for assisting us in the partial data analysis.

Author contributions
ZL, YZ and CW conceived and designed the research. ZL, FD and YZ acquired clinical samples and performed the experiments. ZL performed bioinformatics data analysis. ZL and BL drafted the manuscript. ZL and YZ acquired funding. CW revised the manuscript. All authors have read and approved the final manuscript.

Funding
This work was supported by grants from the National Natural Science Foundation of China (82200290), the China National Postdoctoral Program for Innovative Talents (BX20220094), the China Postdoctoral Science Foundation (2024M752030).

Availability of data and materials
The Circle-Seq and RNA-Seq data in this study can be accessed through GEO series accession numbers GSE241568 and GSE162505.

Declarations

Ethics approval and consent to participate
This study was approved by The Medical Ethics Committee of Zhongshan Hospital of Fudan University (approval number: B2022-267R). The study was conducted in accordance with the guidelines of the Declaration of Helsinki. All informed consent forms were obtained.

Consent for publication
Not applicable.

Competing interests
The authors declare no competing interests.

Author details
[1]Department of Cardiology, Shanghai Ninth People's Hospital, Shanghai Jiao Tong University School of Medicine, Shanghai 200001, China. [2]Department of Cardiology, Affiliated Hospital of Guizhou Medical University, Guiyang 550004, China. [3]Department of Radiology, Renji Hospital, Shanghai Jiao Tong University School of Medicine, Shanghai 200127, China. [4]Key Laboratory of Anesthesiology, Ministry of Education, Shanghai Jiao Tong University, Shanghai 200127, China. [5]Department of Cardiology, Affiliated Hospital of Zunyi Medical University, Zunyi 563099, China. [6]Department of Cardiology, Zhongshan Hospital, Fudan University, Shanghai 200030, China.

Received: 17 September 2024 Accepted: 28 October 2024
Published online: 29 November 2024

References

1. Hotta Y, Bassel A. Molecular size and circularity of DNA in cells of mammals and higher plants. Proc Natl Acad Sci U S A. 1965;53(2):356–62.
2. Cox D, Yuncken C, Spriggs AI. Minute chromatin bodies in malignant tumours of childhood. Lancet. 1965;1(7402):55–8.
3. Wu S, Turner KM, Nguyen N, Raviram R, Erb M, Santini J, Luebeck J, Rajkumar U, Diao Y, Li B, et al. Circular ecDNA promotes accessible chromatin and high oncogene expression. Nature. 2019;575(7784):699–703.
4. Zhu Y, Gujar AD, Wong CH, Tjong H, Ngan CY, Gong L, Chen YA, Kim H, Liu J, Li M, et al. Oncogenic extrachromosomal DNA functions as mobile enhancers to globally amplify chromosomal transcription. Cancer Cell. 2021;39(5):694–707.
5. Luebeck J, Ng AWT, Galipeau PC, Li X, Sanchez CA, Katz-Summercorn AC, Kim H, Jammula S, He Y, Lippman SM, et al. Extrachromosomal DNA in the cancerous transformation of Barrett's oesophagus. Nature. 2023;616(7958):798–805.
6. Verhaak RGW, Bafna V, Mischel PS. Extrachromosomal oncogene amplification in tumour pathogenesis and evolution. Nat Rev Cancer. 2019;19(5):283–8.
7. Koche RP, Rodriguez-Fos E, Helmsauer K, Burkert M, MacArthur IC, Maag J, Chamorro R, Munoz-Perez N, Puiggròs M, Dorado Garcia H, et al. Extrachromosomal circular DNA drives oncogenic genome remodeling in neuroblastoma. Nat Genet. 2020;52(1):29–34.
8. Hull RM, King M, Pizza G, Krueger F, Vergara X, Houseley J. Transcription-induced formation of extrachromosomal DNA during yeast ageing. PLoS Biol. 2019;17(12):e3000471.
9. Qiu GH, Zheng X, Fu M, Huang C, Yang X. The decreased exclusion of nuclear eccDNA: From molecular and subcellular levels to human aging and age-related diseases. Ageing Res Rev. 2021;67:101306.
10. Paulsen T, Shibata Y, Kumar P, Dillon L, Dutta A. Small extrachromosomal circular DNAs, microDNA, produce short regulatory RNAs that suppress gene expression independent of canonical promoters. Nucleic Acids Res. 2019;47(9):4586–96.
11. Wang Y, Wang M, Djekidel MN, Chen H, Liu D, Alt FW, Zhang Y. eccDNAs are apoptotic products with high innate immunostimulatory activity. Nature. 2021;599(7884):308–14.
12. Yang F, Su W, Chung OW, Tracy L, Wang L, Ramsden DA, Zhang ZZZ. Retrotransposons hijack alt-EJ for DNA replication and eccDNA biogenesis. Nature. 2023;620(7972):218–25.
13. Weintraub RG, Semsarian C, Macdonald P. Dilated cardiomyopathy. Lancet. 2017;390(10092):400–14.
14. Hershberger RE, Hedges DJ, Morales A. Dilated cardiomyopathy: the complexity of a diverse genetic architecture. Nat Rev Cardiol. 2013;10(9):531–47.
15. Flores SC, Sunnerhagen P, Moore TK, Gaubatz JW. Characterization of repetitive sequence families in mouse heart small polydisperse circular DNAs: age-related studies. Nucleic Acids Res. 1988;16(9):3889–906.
16. Møller HD, Mohiyuddin M, Prada-Luengo I, Sailani MR, Halling JF, Plomgaard P, Maretty L, Hansen AJ, Snyder MP, Pilegaard H, et al. Circular DNA

elements of chromosomal origin are common in healthy human somatic tissue. Nat Commun. 2018;9(1):1069.
17. Lin Z, Zhao Y, Dai F, Su E, Li F, Yan Y. Analysis of changes in circular RNA expression and construction of ceRNA networks in human dilated cardiomyopathy. J Cell Mol Med. 2021;25(5):2572–83.
18. Gresham D, Usaite R, Germann SM, Lisby M, Botstein D, Regenberg B. Adaptation to diverse nitrogen-limited environments by deletion or extrachromosomal element formation of the GAP1 locus. Proc Natl Acad Sci U S A. 2010;107(43):18551–6.
19. Dillon LW, Kumar P, Shibata Y, Wang YH, Willcox S, Griffith JD, Pommier Y, Takeda S, Dutta A. Production of extrachromosomal microDNAs is linked to mismatch repair pathways and transcriptional activity. Cell Rep. 2015;11(11):1749–59.
20. Carroll SM, DeRose ML, Gaudray P, Moore CM, Needham-Vandevanter DR, Von Hoff DD, Wahl GM. Double minute chromosomes can be produced from precursors derived from a chromosomal deletion. Mol Cell Biol. 1988;8(4):1525–33.
21. Storlazzi CT, Lonoce A, Guastadisegni MC, Trombetta D, D'Addabbo P, Daniele G, L'Abbate A, Macchia G, Surace C, Kok K, et al. Gene amplification as double minutes or homogeneously staining regions in solid tumors: origin and structure. Genome Res. 2010;20(9):1198–206.
22. Cen Y, Fang Y, Ren Y, Hong S, Lu W, Xu J. Global characterization of extrachromosomal circular DNAs in advanced high grade serous ovarian cancer. Cell Death Dis. 2022;13(4):342.
23. Zou S, Chen S, Rao G, Zhang G, Ma M, Peng B, Du X, Huang W, Lin W, Tian Y, et al. Extrachromosomal circular MiR-17-92 amplicon promotes HCC. Hepatology. 2024;79(1):79–95.
24. Shibata Y, Kumar P, Layer R, Willcox S, Gagan JR, Griffith JD, Dutta A. Extrachromosomal microDNAs and chromosomal microdeletions in normal tissues. Science. 2012;336(6077):82–6.
25. Zhu J, Zhang F, Du M, Zhang P, Fu S, Wang L. Molecular characterization of cell-free eccDNAs in human plasma. Sci Rep. 2017;7(1):10968.
26. Vogt N, Lefèvre SH, Apiou F, Dutrillaux AM, Cör A, Leuraud P, Poupon MF, Dutrillaux B, Debatisse M, Malfoy B. Molecular structure of double-minute chromosomes bearing amplified copies of the epidermal growth factor receptor gene in gliomas. Proc Natl Acad Sci U S A. 2004;101(31):11368–73.
27. Wang RC, Smogorzewska A, de Lange T. Homologous recombination generates T-loop-sized deletions at human telomeres. Cell. 2004;119(3):355–68.
28. Møller HD, Parsons L, Jørgensen TS, Botstein D, Regenberg B. Extrachromosomal circular DNA is common in yeast. Proc Natl Acad Sci U S A. 2015;112(24):E3114–22.
29. Lv W, Pan X, Han P, Wang Z, Feng W, Xing X, Wang Q, Qu K, Zeng Y, Zhang C, et al. Circle-Seq reveals genomic and disease-specific hallmarks in urinary cell-free extrachromosomal circular DNAs. Clin Transl Med. 2022;12(4):e817.
30. Møller HD, Larsen CE, Parsons L, Hansen AJ, Regenberg B, Mourier T. Formation of extrachromosomal circular DNA from long terminal repeats of retrotransposons in saccharomyces cerevisiae. G3 (Bethesda). 2015;6(2):453–62.
31. Ginno PA, Lott PL, Christensen HC, Korf I, Chédin F. R-loop formation is a distinctive characteristic of unmethylated human CpG island promoters. Mol Cell. 2012;45(6):814–25.
32. Loomis EW, Sanz LA, Chédin F, Hagerman PJ. Transcription-associated R-loop formation across the human FMR1 CGG-repeat region. PLoS Genet. 2014;10(4):e1004294.
33. Sin STK, Jiang P, Deng J, Ji L, Cheng SH, Dutta A, Leung TY, Chan KCA, Chiu RWK, Lo YMD. Identification and characterization of extrachromosomal circular DNA in maternal plasma. Proc Natl Acad Sci U S A. 2020;117(3):1658–65.
34. Kumar P, Dillon LW, Shibata Y, Jazaeri AA, Jones DR, Dutta A. Normal and cancerous tissues release extrachromosomal circular DNA (eccDNA) into the circulation. Mol Cancer Res. 2017;15(9):1197–205.
35. Decout A, Katz JD, Venkatraman S, Ablasser A. The cGAS-STING pathway as a therapeutic target in inflammatory diseases. Nat Rev Immunol. 2021;21(9):548–69.

Publisher's Note